DOI: 10.61782/fa.2023.1089

# EXPERIMENTAL DEVELOPMENT OF A TIMBER FLOOR SYSTEM WITH IMPROVED IMPACT SOUND INSULATION IN THE LOW-FREQUENCY RANGE

**Robin Hierl**[1*] **Ulrich Schanda**[1] **Fabian Schöpfer**[1] **Yvonne Weise**[1]
[1] Laboratory for Sound Measurement, Technical University of Applied Sciences Rosenheim, Germany

### ABSTRACT

As part of a development project with an industrial partner the vibroacoustic characteristics of a timber floor system with a cross-laminated timber ribbed module base floor are experimentally investigated at the Laboratory for Sound Measurement (LaSM) at the Technical University of Applied Sciences Rosenheim (THRO) with the focus on the low frequency range below 200 Hz. The laboratory mock-up is designed in a rather flexible way in order to detach and change individual layers of the floor construction, i.e. the screed, the base-floor and the ceiling. This allows a systematic improvement of each layer by investigating resonance frequencies, damping and operational vibration modes. The aim is to combine sound insulation and sound absorption measures (e.g. Helmholtz resonator) such that low-frequency structural resonances are damped to reduce impact sound in this frequency range.

This paper introduces this project and gives an overview of the laboratory mock-up and the experimental methods. Further steps will include the development of numerical models based on the experimental work.

**Keywords:** *low-frequency impact sound, timber floor, Helmholtz resonator*

***Corresponding author**: *robin.hierl@th-rosenheim.de.*


## 1. INTRODUCTION

Occupants often identify impact sound from people walking as the most disturbing noise source in apartment buildings, e.g. [1, 2]. It is common sense that the reason is due to fact, that the dominant exitation of the floors happens in the low frequency range in coincidence with low impact sound insulation inherent in building constructions. Requirements in many international standards do not cover this frequency range of the occupants' audial impressions [3]. However for higher comfort requirements inhabitants expect a very good impact sound insulation, which can be characterised by a limit on the weighted, normalised impact sound level in combination with a spectrum adaptation term of $L_{\mathrm{n,w}} + C_{\mathrm{I}} < 47\,\mathrm{dB}$, as it is e.g. mentioned in the latest sound insulation manual of Informationsdienst Holz for Germany [4, 5]. For this project a value of $L_{\mathrm{n,w}} + C_{\mathrm{I}} < 40\,\mathrm{dB}$ was specified as achievement. The existing timber floor construction [6] has been measured as $L_{\mathrm{n,w}} + C_{\mathrm{I}} = 40 + 8$ dB.

The aim of the project is the development of a new type of cross-laminated timber floor with a visible wooden ceiling, which is directly attached to the base floor. The development does include the possibility to integrate advanced measures like Helmholtz resonators or tuned-mass dampers to damp or minimise low-frequency structural resonances [7]. For the optimisation of the floor system detailed investigations in the measurements of eigenmodes (normal modes) using operational modal analysis is compulsory, since the eigenmodes in the low frequency range are certainly dominating the low-frequency impact sound due to the low mode density.

The experimental development will be accompanied at a later stage by a finite element-based simulation and calculation program designed specifically for the system in order to predict the impact sound level in each building-specific layout in the planning process. A FE-model has to be validated by experimental results on the eigenfrequencies (normal frequencies) and the eigenmodes of the system. The validation approach has been described in earlier research projects, e.g. [8, 9].

## 2. THE TIMBER FLOOR SYSTEM

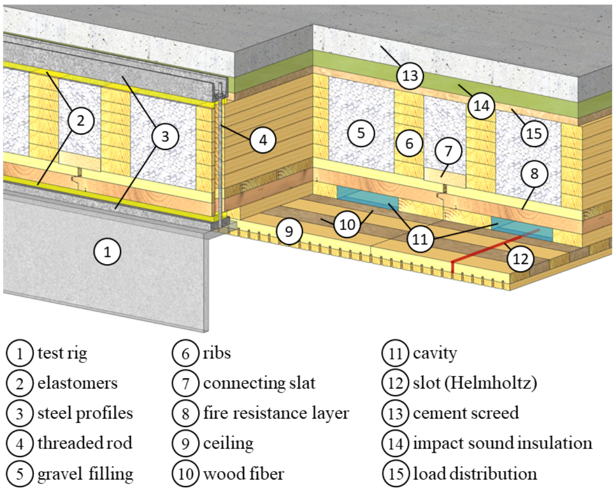


**Figure 1**: Floor structure and bearing in the test rig

Figure 1 includes a detailed drawing of the floor system. For the purpose of the experimental analysis, the floor system is basically divided into the upper floor, the base floor and a directly attached ceiling which is part of the load-bearing cross section.

The upper floor structure is replaceable and consists of a panel for load distribution out of wood fibre, impact sound insulation out of glass wool and a floating cement screed (see Figure 1, Nos. 13-15).

The base floor consists of several cross-laminated timber ribbed modules of a width of 625 mm. The sustainability aspect is addressed due to a comparatively high simplicity with respect on material and production. The elements themselves include three load-bearing ribs as well as a solid cross-laminated timber fire resistance layer (see Figure 1, Nos. 6, 8). They are connected via groove and tongue and a connecting slat above the joint (see Figure 1, No. 7). The elements are prefabricated, then transported and put together at the building site. Limestone gravel fillings are optionally applied in the spaces between the ribs as additional mass (see Figure 1, No. 5).

The ceiling consists of acoustic panels with a visible wooden surface and a back side with wood fibre parts (see Figure 1, Nos. 9, 10). Additional bars at the underside of the base floor create space for installations and increase sound absorption (see Figure 1, No. 11). The ceiling is usually assembled and attached to the base floor in the factory as well. For the investigations of this project, also the ceiling is designed as an exchangeable layer. The suspension height and therefore the cavity behind the ceiling can be variably adjusted by adding further additional bars.

## 3. FLOOR MOUNTING IN THE TEST RIG

The bearing of the base floor is realised along the short sides (2,7 m) in the test rig. Steel profiles are attached to the top and bottom of the elements, connected with pre-tensioned threaded rods M6 each 20 cm (see Figure 1, Nos. 3, 4). The rods pass through holes in the base floor without any contact to the base floor. Between the steel profiles, elastomers are used in order to realise simply supported boundary conditions (see Figure 1, No. 2). The steel profiles allow an adjustment of the line load over the entire width of the base floor. The elastomers out of Sylomer SR 450 are selected in a way that no disturbing influences on the behavior of the elements are expected in the range of low frequencies below 15 Hz. However in the context of an accurate modelling of the boundary conditions, it is expected that the elastomer has a significant influence on the support impedance and so on the result of the simulation [10]. Along its long sides (5,5 m) the base floor is free.

**Figure 2**: Example of sealing with TEROSON® RB IX

To prevent any transmission of airborne sound during the measurement of the impact sound level, the kneadable butyl sealant TEROSON® RB IX is used (see Figure

2) in order to avoid any sound transmission through slits etc. Measurements of the eigenmodes have shown, that the sealant unfortunately has a big impact on the eigenmodes and eigenfrequencies. This was not at all expected; the results are addressed in Chapter 6.

To make the floor structure removeable, a cement screed with a high bending tensile strength and additional reinforcement is used in order that it can be lifted in and out of the test rig using a crossbeam. As Figure 3 shows, the cement screed is divided into three individual parts. The separation into three parts was necessary due to a limited capacity of the crane in the laboratory.

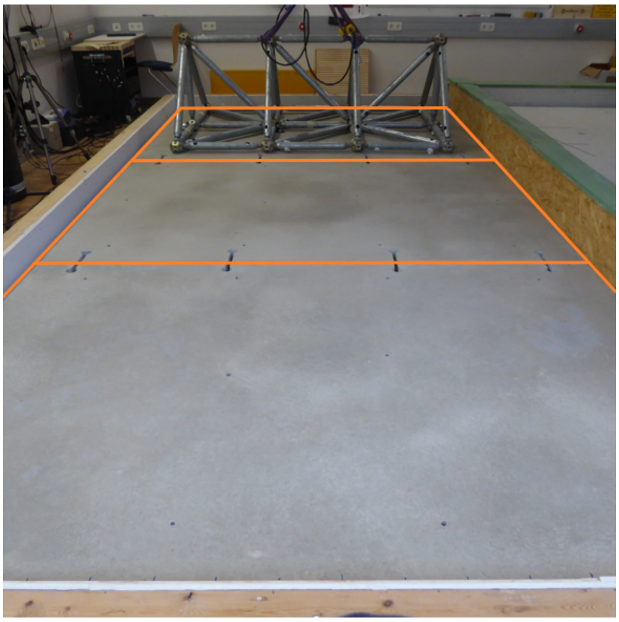

**Figure 3**: Three-part cement screed (orange) and crossbeam in the test rig

Studies have shown that the length and width of floating cement screeds influence the impact of sound reduction $\Delta L_\text{w}$. For screed slabs with a thickness of less than $70\,\text{mm}$, a relevant increase in impact sound reduction can be seen below an area of $4\,\text{m}^2$ to $5\,\text{m}^2$. [11]

With a selected thickness of $50\,\text{mm}$, a minimum size of the screed elements of $5\,\text{m}^2$ was chosen, resulting in a division of the cement screed for the test rig into three parts. The parts can be attached to each other where they face each other by heavy-load connectors.

The effect of the partitioning of the screed on the low-frequency impact sound insulation is also addressed in Chapter 6.

## 4. MEASUREMENT METHOD

For the operational modal analyses, the base floor or screed is excited with a modal shaker. The excitation is done via an adapted logarithmic sine sweep, which excites the floor over the frequency of $3\,\text{Hz}$ to $210\,\text{Hz}$ in $30\,\text{s}$.

The excitation position is chosen that no node of the first modes is present and that as many eigenmodes of the construction as possible are activated. On the one hand, a adequate distance to the bearing is necessary to stimulate the ceiling sufficiently. On the other hand, the position is close enough to the edge to have a clearance to the first vibration nodes of the modes of interest. The schematic Figure 4 shows the amplitude of the oscillation of the first 10 modes with jointed bearings on both sides. The positions with adequate excitation of all displayed modes (all normalised amplitudes $A \geq 0.15$) are shown in purple on the X-axis. In the area $0.27\,\text{m}$ to $0.49\,\text{m}$ from the support, a suitable excitation range is guaranteed. For the modal analysis, the excitation position near the maximum within this range at $0.45\,\text{m}$ is selected, since at this point the first modes with still low amplitude can be sufficiently excited. To prevent disturbing resonances of the shaker setup, the shaker is connected to a chain suspension with additional weight (see Figure 5). Using accelerometers or a laser Doppler vibrometer, transfer functions are measured between the excitation position and individual measuring points in a measuring grid of $30\,\text{cm}$ to $40\,\text{cm}$. Usually 117 measurement points are used for averaging to one transfer function (see Figure 8). With the measured transfer functions, three-dimensional vibration images are generated over the frequency in MATLAB®.

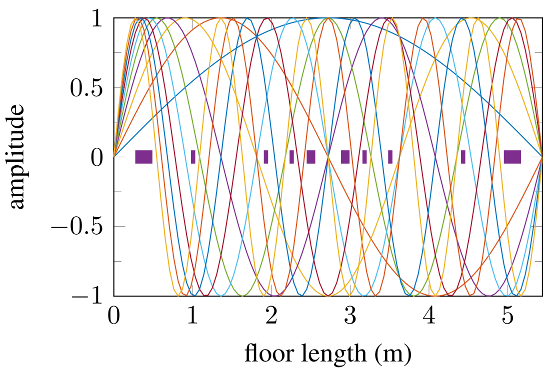


**Figure 4**: Oscillation of the first 10 modes in the longitudinal axis of the floor

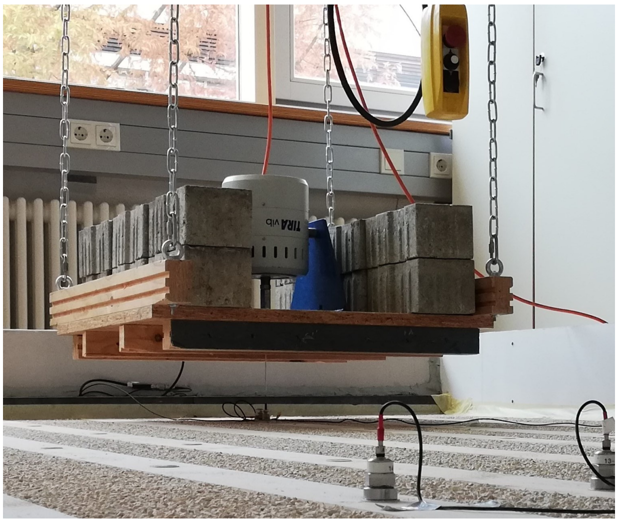

**Figure 5**: Modal shaker on a chain suspension and accelerometers mounted on the base floor

## 5. HELMHOLTZ RESONATORS

Preceding investigations using impedance tube measurements especially designed for the low-frequency range proved the possibility of integration of Helmholtz resonators in the ceiling. One test specimen is shown in Figure 6. For this purpose, the cavity behind the profile

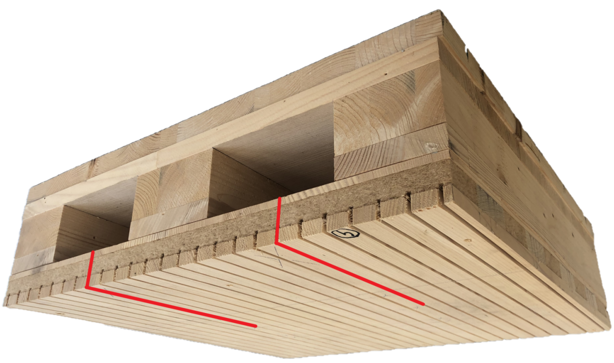

**Figure 6**: Helmholtz test specimen with slots in red

is divided lengthwise into chambers. Each chamber is equipped with the profile slotted once (see also Figure 1, No. 12). Via the parameter of slot length and cavity depth, the resonator is precisely adjustable to a narrow-band frequency range. A special, well-optimised damping layer is included. In Figure 7 the sound absorption of Helmholtz absorber with a constant cavity and different slot lengths

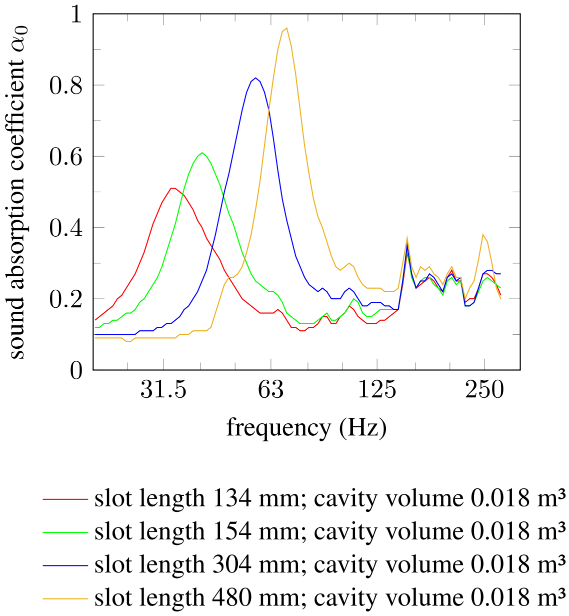


**Figure 7**: Sound absorption of Helmholtz absorbers with variable slot lengths

is shown. If the air volume remains the same, but the slot is enlarged, the resonant frequency moves to higher frequencies. In addition, the characteristic of the absorber becomes more narrow-band with a higher maximum absorption as expected. Further investigations showed that also in the range of the suspended height below $0.20\,\mathrm{m}$, the Helmholtz resonator is functioning. Based on this, the effect of the Helmholtz resonator on the complete floor structure will be analysed in future experimental investigations.

## 6. FIRST EXPERIMENTAL RESULTS

### 6.1 Boundary conditions

Measurements show that the sealant on the long, non-bearing sides of the floor has an influence on the eigenfrequencies, the damping, and, above all the vibration modes during the operational modal analysis (see Figure 8). Without sealing, the mode density is higher and the damping of the eigenfrequencies is lower. In the sealed state the eigenmode with the lowest frequency shows the behaviour of a bending mode with vibration nodes on the longitudinal and transverse sides. Removing the sealant the first mode is a torsional mode with free edges on the

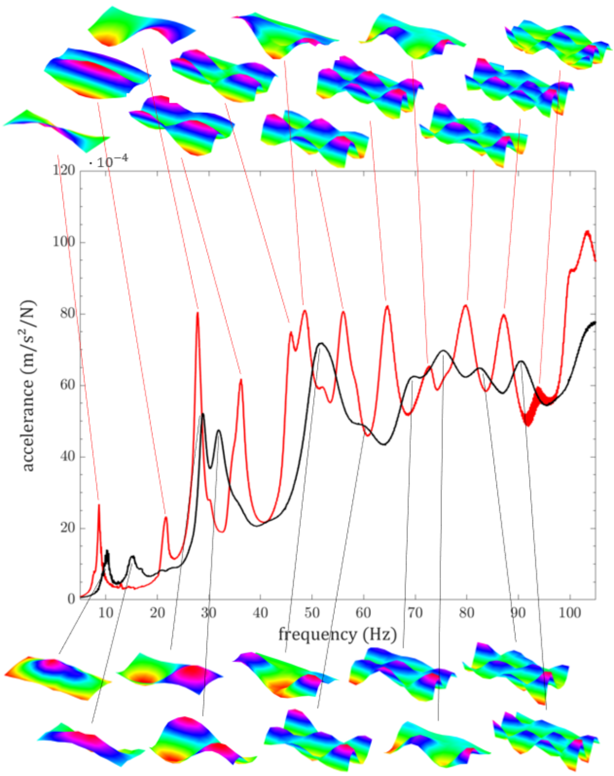


**Figure 8**: Transfer function base floor with (black)/ without (red) sealant

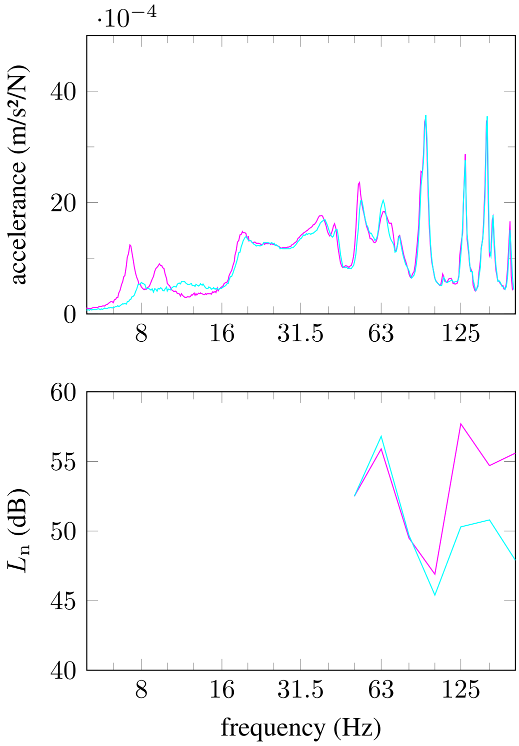


**Figure 9**: Modal analyses and impact sound measurement with optimised (blue)/ without (magenta) sealant

long side.

However for the understanding of the relation of impact sound level at low frequencies and the contributing eigenmodes the measurements have to be done with the same system, otherwise an optimisation does not seem feasible. Therefore a compromise between sealing measures, which are minimised to maintain simple and reproducible boundary conditions and sufficient sealing in order to minimise impact sound level by flanking airborne sound paths through slits is necessary.

In Figure 9, the accelerance without and with optimised sealing on the base floor with additional mass loading is shown in the upper graph. The lower graph shows the values of the impact sound measurement up to 200 Hz. The impact sound levels show that increased values occur from 100 Hz without sealing. They are due to the flanking airborne sound paths via the screed face into the existing joint (see Figure 10). The improved sealing reduces this influence and changes the accelerance only below 16 Hz. This range is not relevant for the acoustic optimisation of the ceiling. However, it should be noted that sealing measures can have influence on the vibration serviceability of wooden floors since there exist requirements according to [12].

### 6.2 Additional mass loading

Analyses of the base floor with and without limestone gravel reveal a shift of the eigenfrequencies by a factor of 0.54 towards lower frequencies (additional mass $143\,\mathrm{kg/m^2}$, + 43 % compared to original surface mass). Figure 11 shows the comparison of the structure with and without filling. This reduction considered in the frequency range up to 100 Hz results from the fact that the filling can be evaluated acoustically simply as mass without any additional stiffness. The base floor is excited less by an increase in mass, and the damping also increases with the addition of the filling.

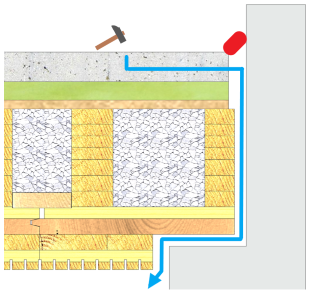

**Figure 10**: Gap between the test rig and floor creates a secondary sound transmission path (blue); sealing (red)

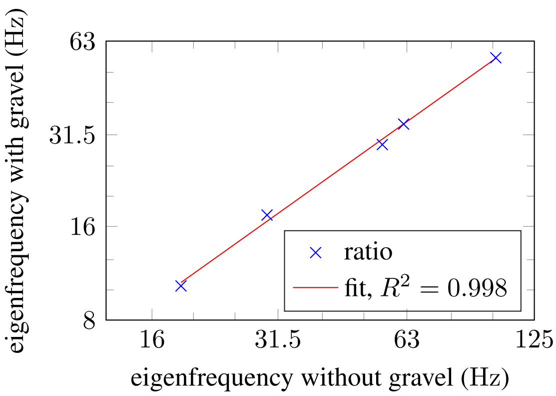


**Figure 11**: Comparison of eigenfrequencies of the same mode of the base floor with and without limestone gravel as additional mass loading

### 6.3 Partitioning of the screed

Figure 12 shows the influence of the partitioning of the screed into three parts on the normalised impact sound pressure level. Two measurements in the lab are compared, one with the parts of the screed attached together by integrated heavy-load connectors, the other with completely detached parts of the screed. Both measurements show rather the same impact sound insulation in the frequency range of interest. Comparing these measurements with the impact sound insulation of a floor measured in a building with the identical floor construction, the spectral shape below 100 Hz is rather the same except that the large timber floor in the building does show much higher impact sound pressure levels in the 50 Hz 1/3-octave band. The reason for the much lower impact sound levels at 125 Hz and higher is still part of the ongoing investigations.

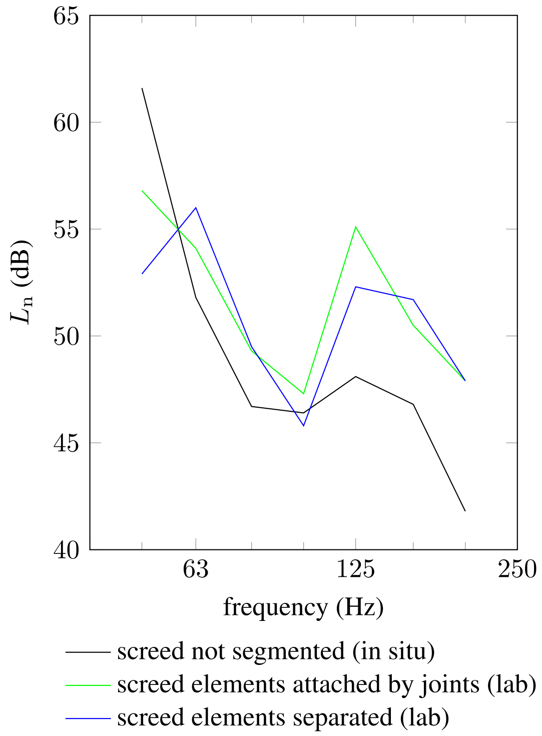


**Figure 12**: Effect of the partitioning of the screed on the impact sound level

## 7. OUTLOOK

In the context of further investigations, the ceiling, including the Helmholtz resonator, is examined in the test rig. The question here is to what extent the impact sound of the floor in the low-frequency range can be improved by the design of the Helmholtz resonator, by also taking into account the room acoustic effect as an absorber.

After the implementation of all layers (including the ceiling and upper floor) in the FE modelling, variations of the structure are added to the model with validation via vibroacoustic measurements. These are the basis for the calculation tool, which is being developed specifically to design the cross-laminated timber ribbed module with reduced low-frequency structural resonances and impact sound fitted for the individual type of the building project.

## 8. REFERENCES


[1] J. Y. e. a. Jeon, "A quantification model of overall dissatisfaction with indoor noise environment in residential buildings.," *Applied Acoustics*, vol. 71, pp. 914–921, 2010.

[2] B. Zeitler, M. Schneider, C. Höller, and U. Schanda, "Tieffrequenter Trittschall – Stand der Wissenschaft und Technik," in *Fortschritte der Akustik - DAGA* (Deutsche Gesellschaft für Akustik e.V., ed.), 2020.

[3] B. Rasmussen, "Sound insulation between dwellings – comparison of national requirements in europe and interaction with acoustic classification schemes," in *Proceedings of ICA 2019*, 2019.

[4] A. Blödt, A. Rabold, and M. Halstenberg, "Schallschutz im Holzbau: Grundlagen und Vorbemessung: Holzbauhandbuch, Reihe 3, Teil 3, Folge 1."

[5] A. Rabold and U. Schanda, "Prediction method to prove requirements on impact sound insulation of timber floors with special consideration of low frequencies," in *Proceedings of ICSV 2021*, 2021.

[6] "*https://www.lignotrend.com/en/products/construction /floor-slabs*."

[7] U. Schanda, "Resonant system for the absorption of low frequency impact noise and for the damping of low frequency vibrations," in *Proceedings of Forum Acusticum 2011*, 2011.

[8] M. Kohrmann, M. Buchschmid, G. Müller, R. Völtl, and U. Schanda, "Numerical models for the prediction of vibro-acoustical characteristics of light-weighted ceilings," in *Proceedings of Inter-Noise 2013*, 2013.

[9] C. Hopkins, M. Filippoupolitis, N. Ferreira, R. Völtl, U. Schanda, J. P. Mahn, and L. Krajci, "Vibroacoustic finite element modelling of the low-frequency performance of a solid timber floor formed from dowel-connected joists," in *Proceedings of Inter-Noise 2016*, 2016.

[10] M. Kohrmann, R. Völtl, G. Müller, U. Schanda, and M. Buchschmid, "Planungshilfen zur schall- und schwingungstechnischen Beschreibung von Holzdecken und zur Bewertung und Dimensionierung von angepassten Schwingungsschutzsystemen: Abschlussbericht zum AiF Forschungsvorhaben VibWood," 2014.

[11] D. Erler, D. Sprinz, and J. Hübelt, "Abhängigkeit der Trittschallminderung schwimmender Estriche von der Estrichfläche," in *Fortschritte der Akustik - DAGA* (Deutsche Gesellschaft für Akustik e.V., ed.), 2017.

[12] DIN EN 1995-1-1:2010-12, "Eurocode 5: Bemessung und Konstruktion von Holzbauten: Teil 1-1: Allgemeines - Allgemeine Regeln und Regeln für den Holzbau: Deutsche Fassung EN 1995-1-1:2004 + AC:2006 + A1:2008."